Rare Metal Materials and Engineering
Volume 51, Issue 9, September 2022
Available online at www.rmme.ac.cn

Science Press

Cite this article as: Cheng Juan, Liu Cuilan, Zhang Guangrui, et al. Magnetic Properties of Mix-Bonded $La_{0.8}Ce_{0.2}Fe_{11.7-x}Mn_xSi_{1.3}H_{1.8}$ Magnetic Refrigerants[J]. Rare Metal Materials and Engineering, 2022, 51(09): 3153-3158.

ARTICLE

Magnetic Properties of Mix-Bonded $La_{0.8}Ce_{0.2}Fe_{11.7-x}Mn_xSi_{1.3}H_{1.8}$ Magnetic Refrigerants

Cheng Juan[1], Liu Cuilan[1], Zhang Guangrui[1], Sun Naikun[2], Zhang Yingde[1], Jin Peiyu[1], Huang Jiaohong[1]

[1] State Key Laboratory of Baiyunobo Rare Earth Resource Researches and Comprehensive Utilization, Baotou Research Institute of Rare Earths, Baotou 014030, China; [2] School of Science, Shenyang Ligong University, Shenyang 110159, China

Abstract: $La_{0.8}Ce_{0.2}Fe_{11.7-x}Mn_xSi_{1.3}$ master alloys were prepared by medium frequency induction furnace, then annealed, saturatedly hydrogenated, and finally crushed into powders. The multiple components of $La_{0.8}Ce_{0.2}Fe_{11.7-x}Mn_xSi_{1.3}H_{1.8}$ (x=0.23, 0.26, 0.29, 0.32, wt%) powders with the Curie temperature (T_C) interval of 5 K were mix-bonded by epoxy resin to extend the full width at half maximum of magnetic entropy of alloy. The magnetic properties of the mix-bonded specimens were measured by VersaLab and adiabatic temperature change direct test device. The maximal magnetic entropy change of the mix-bonded specimens is decreased, whereas the full width at half maximum of magnetic entropy and the relative cooling power are increased, compared with those of the single-component-bonded specimens. The maximal relative cooling power is 139.2 J/kg for the four-component-bonded specimen.

Key words: magnetic materials; magnetocaloric effect; relative cooling power; rare earths

As La(Fe, Si)$_{13}$ materials have characteristics of large magnetocaloric effect, continuously adjustable Curie temperature (T_C), and low cost, they are regarded as one of the most promising magnetocaloric materials for room-temperature refrigeration[1-3]. However, T_C of the La(Fe, Si)$_{13}$ parent alloys is too low for room temperature magnetic refrigeration[3]. Although T_C of La(Fe, Si)$_{13}$ materials can increase to room temperature by partial substitution of Co for Fe, their magnetocaloric effect decreases sharply and the magnetic phase transition changes from the first-order to second-order[4]. It is found that after hydrogen absorption, the T_C of La(Fe, Si)$_{13}$ materials is increased and the large magnetocaloric effect of first-order transition remains[5-10]. Unfortunately, the application of La(Fe, Si)$_{13}H_y$ materials in magnetic refrigerator is restricted due to their poor mechanical properties and narrow full width at half maximum of magnetic entropy (ΔT). In order to improve the mechanical properties, Zhang et al[11] prepared the epoxy resin-bonded $LaFe_{11.7}Si_{1.3}C_{0.2}H_{1.8}$ material and found that the maximal compressive strength of 162 MPa is achieved when the content of epoxy resin is 3wt%. Pan et al[12] bonded the La(Fe, Si)$_{13}$ hydrides with sodium silicate. Besides, the low melting point metals, such as Sn[13], In[14,15], Pb-Bi-Cd[15], and $Bi_{32.5}Sn_{16.5}In_{51}$[16], have been widely used as the metal adhesive to bond the La(Fe, Si)$_{13}$ hydrides. However, the broadening of the ΔT of La(Fe, Si)$_{13}$ hydrides is rarely studied.

In this research, various $La_{0.8}Ce_{0.2}Fe_{11.7-x}Mn_xSi_{1.3}H_y$ alloys of the first-order phase transition with the Curie temperature interval of 5 K were mix-bonded by epoxy resin to expand the ΔT. The magnetic properties of the composites were investigated.

1 Experiment

The industrially pure raw materials (99.5wt% La, 99.5wt% Ce, 99wt% Fe, 99.7wt% Mn, 99.9wt% Si) were cast to prepare the $La_{0.8}Ce_{0.2}Fe_{11.7-x}Mn_xSi_{1.3}$ master alloys by medium frequency induction furnace. Afterwards, the alloys were annealed at 1363 K for 144 h in Ar atmosphere. The bulk alloys were crushed into irregular particles and hydrogenated in a hydrogen atmosphere of 0.13 MPa at 593 K for 5 h until

Received date: September 23, 2021
Foundation item: National Natural Science Foundation of China (52066001); Natural Science Foundation of Inner Mongolia Autonomous Region (2021MS05016); Northern Rare Earth Project (BFXT-2021-D-0013)
Corresponding author: Huang Jiaohong, Ph. D., Professor, State Key Laboratory of Baiyunobo Rare Earth Resource Researches and Comprehensive Utilization, Baotou Research Institute of Rare Earths, Baotou 014030, P. R. China, Tel: 0086-472-5179269, E-mail: jiaohongh@163.com

they were hydrogen-saturated. Then the $La_{0.8}Ce_{0.2}Fe_{11.7-x}Mn_xSi_{1.3}H_{1.8}$ alloys were obtained and subsequently ground into powders with particle size<0.15 mm. All the powders consisting of different components were bonded by 1.8wt% epoxy resin, then pressed into cylinders at the pressure of 557 MPa, and finally annealed at 175 °C for 45 min. The $La_{0.8}Ce_{0.2}Fe_{11.7-x}Mn_xSi_{1.3}H_{1.8}$ alloys with Mn contents of x= 0.23, 0.26, 0.29, 0.32 (wt%) are denoted as specimen A, B, C, and D, respectively. The composition of mix-bonded $La_{0.8}Ce_{0.2}Fe_{11.7-x}Mn_xSi_{1.3}H_{1.8}$ alloys is listed in Table 1.

The phase components of specimens were determined by X-ray diffraction (XRD). The magnetic properties were measured by VersaLab with VSM option, and the magnetic entropy changes were calculated by Maxwell relation. The adiabatic temperature changes were tested by the home-made adiabatic temperature change direct test device. The compressive strength was tested by the electronic universal testing machine (WDW3200).

Table 1 Components of mix-bonded $La_{0.8}Ce_{0.2}Fe_{11.7-x}Mn_xSi_{1.3}H_{1.8}$ alloys (wt%)

Mix-bonded specimen	Component				Epoxy resin
	A	B	C	D	
M_{AB}	49.10	49.10	-	-	1.8
M_{BC}	-	49.10	49.10	-	1.8
M_{CD}	-	-	49.10	49.10	1.8
M_{ABC}	32.73	32.73	32.73	-	1.8
M_{BCD}	-	32.73	32.73	32.73	1.8
M_{ABCD}	24.55	24.55	24.55	24.55	1.8

2 Results and Discussion

Fig. 1 shows the XRD patterns of $La_{0.8}Ce_{0.2}Fe_{11.7-x}Mn_xSi_{1.3}H_{1.8}$ alloys with x=0.23, 0.26, 0.29, 0.32. It can be seen that all the specimens have the main cubic phase of $NaZn_{13}$ structure, and a small amount of impurity phase α-Fe can be detected.

Fig. 2 shows the relationship between the magnetization M and temperature T of various $La_{0.8}Ce_{0.2}Fe_{11.7-x}Mn_xSi_{1.3}H_{1.8}$ alloys at the magnetic field of 0.05 T in the warming process. The T_C is obtained by the valley bottom values of dM/dT-T curves. It is known that the T_C of $La(Fe_xSi_{1-x})_{13}$ alloys can be reduced through the partial substitution of Mn for Fe or Ce for La[17], so the T_C of $La_{0.8}Ce_{0.2}Fe_{11.7-x}Mn_xSi_{1.3}H_{1.8}$ alloys is relatively lower than that of $La(Fe, Si)_{13}H_{1.8}$ alloy. The T_C interval of specimen A, B, C, and D is 5 K, as listed in Table 2. The specimen M_{ABC} and M_{BCD} both show the distinctive magnetic transitions. In order to further widen the half peak width of the

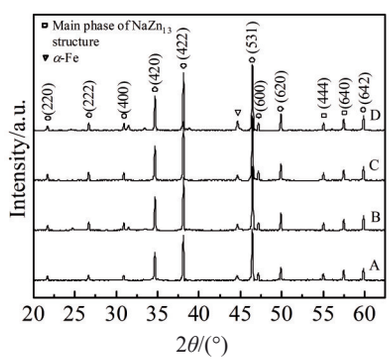

Fig.1 XRD patterns of specimen A, B, C, and D at room temperature

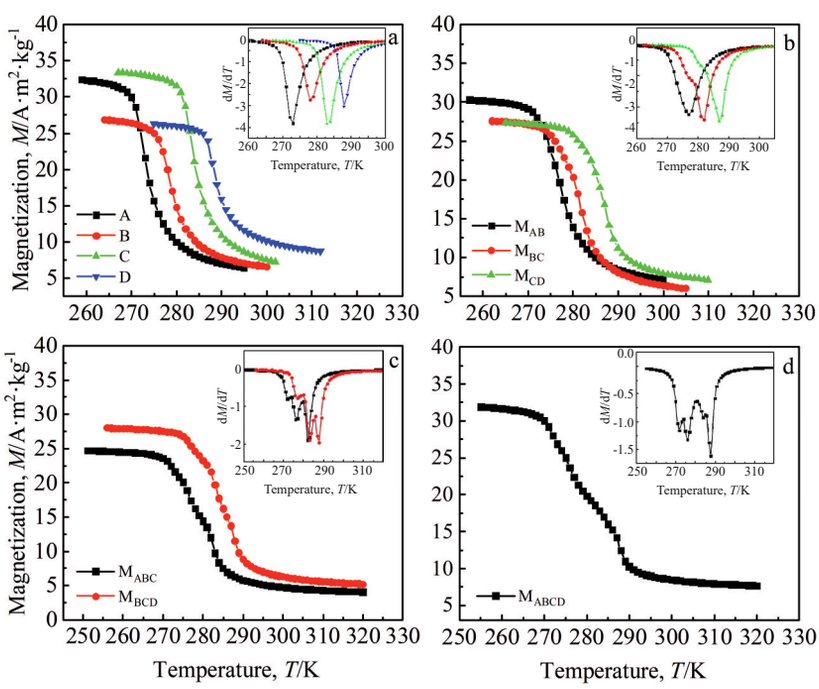

Fig.2 Relationships between magnetization and temperature of different specimens: (a) single-component specimens A~D; (b) two-component-bonded specimens M_{AB}, M_{BC}, and M_{CD}; (c) three-component-bonded specimens M_{ABC} and M_{BCD}; (d) four-component-bonded specimen M_{ABCD}

Table 2 Magnetic transition temperatures T_C of different $La_{0.8}Ce_{0.2}Fe_{11.7-x}Mn_xSi_{1.3}H_{1.8}$ alloy specimens (K)

A	B	C	D	M_{AB}	M_{BC}	M_{CD}	M_{ABC}	M_{BCD}	M_{ABCD}
273	278	283	288	277	282	287	276, 282	283, 288	272, 276, 283, 287

magnetization of alloys, specimen A, B, C, and D are mix-bonded, and therefore four magnetic transition points can be observed for the specimen M_{ABCD}, which are basically consistent with those of the single-component-bonded specimen A, B, C, and D.

The area of magnetic phase transition from the ferromagnetic state to the paramagnetic state of the mix-bonded specimens is larger than that of the single-component-bonded specimens, indicating that the maximal magnetic entropy change of the mix-bonded specimens reduces, compared with that of the single-component-bonded specimens. With increasing the components in mix-bonded specimens, the temperature range of magnetic phase transition becomes wider, and the maximum magnetic entropy change is decreased.

Fig. 3 exhibits the magnetization isotherms and the corresponding Arrott plots of different $La_{0.8}Ce_{0.2}Fe_{11.7-x}Mn_x$-$Si_{1.3}H_{1.8}$ alloys. According to the magnetization isotherms, there is no obvious change of magnetic moments for the single-component-bonded specimens. The magnetic moment changes more and more slowly with increasing the magnetic field for the two-component-bonded specimens, implying that the field-induced first-order phase transition is weakened and a smaller hysteresis of 2.68 J/kg is achieved, compared with that of the single-component-bonded specimens (3.66 J/kg for specimen C; 5.15 J/kg for specimen D). It is found that the hysteresis caused by the magnetic field cycles can reduce the refrigeration capacity[18]. Hence, the reduction in hysteresis for the mix-bonded specimens is favorable for the magnetic refrigeration. According to the s-d orbit of electrons, the slop of the Arrott plots can be used to describe the types of the magnetic phase transition. If the slop is positive, the phase transition is second-order; if the slop is negative or the inflection point exists, the phase transition is first-order[19]. The Arrott plots in Fig. 3d and 3e have obvious inflection points, indicating that the field-induced first-order phase transition occurs. The inflection point in Fig.3f is not obvious, indicating that the first-order phase transition is weakened in the two-component-bonded specimen M_{CD}.

The maximum magnetic entropy ΔS_M of mix-bonded specimens at the magnetic strength of 0~2 T can be calculated based on the isothermal magnetization curves by Maxwell relation[20], as follows:

$$\Delta S_M(T,H) = \int_0^H (\partial M/\partial T)_H \mathrm{d}H \quad (1)$$

where T is the temperature; H is the magnetic field intensity; M is the magnetization. Table 3 shows the calculation results of maximum magnetic entropy of different $La_{0.8}Ce_{0.2}$-$Fe_{11.7-x}Mn_xSi_{1.3}H_{1.8}$ alloys. The maximal magnetic entropy changes of all the mix-bonded specimens are decreased, compared with those of the single-component-bonded specimens. The average ΔS_M of two-component-bonded

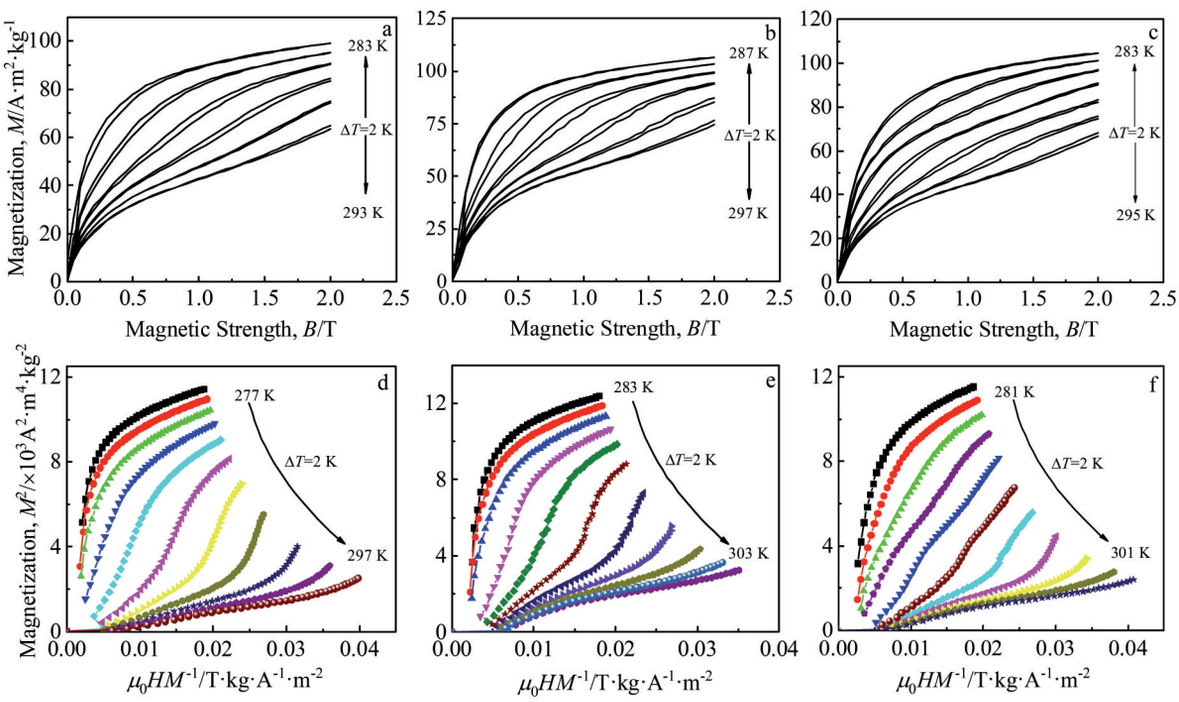

Fig.3 Isothermal magnetization curves at magnetic strength of 0~2 T (a~c) and Arrott plots (d~f) of specimen C (a, d), specimen D (b, e), and specimen M_{CD} (c, f)

Table 3 ΔS_M, ΔT, and RCP of different $La_{0.8}Ce_{0.2}Fe_{11.7-x}Mn_xSi_{1.3}H_{1.8}$ alloy specimens

Specimen	A	B	C	D	M_{AB}	M_{BC}	M_{CD}	M_{ABC}	M_{BCD}	M_{ABCD}
$-\Delta S_M$/J·kg^{-1}·K^{-1}	8.96	8.62	9.33	8.88	7.91	8.61	8.53	7.10	7.47	5.80
ΔT/K	12.5	12.7	12.3	11.0	15.0	13.6	14.5	19.0	18.0	24.0
T_1/K	270.0	275.0	280.3	286.0	272.0	276.4	282.5	270.0	277.0	270.3
T_2/K	282.5	287.7	292.6	297.0	287.0	290.0	296.0	289.0	295.0	294.3
RCP/J·kg^{-1}	112.00	109.47	114.76	97.71	118.64	117.1	123.67	134.83	134.46	139.20

specimens, three-component-bonded specimens, and four-component-bonded specimens is decreased by about 6.7%, 18.6%, and 35.2%, compared with that of the corresponding single-component-bonded specimens, respectively. The decreased ΔS_M of the mix-bonded specimens is caused by the weakening of the magnetic transformation.

In order to further study the refrigeration capacity of the materials, the relative cooling power (RCP) is calculated by Eq.(2), as follows:

$$RCP = -\Delta S_M \Delta T \quad (2)$$

where $\Delta T=T_2-T_1$ (the values of T_1 and T_2 are listed in Table 3). Although the ΔS_M of the mix-bonded specimens decreases, compared with that of the single-component-bonded specimens, RCP of the mix-bonded specimens is higher than that of all the single-component-bonded specimens as a result of the broadening of ΔT. The average RCP of two-component-bonded, three-component-bonded, and four-component-bonded specimens increases by 10.4%, 24.1%, and 28.3%, compared with that of the single-component-bonded specimens, respectively. In addition, RCP of the four-component-bonded specimen is the largest of 139.20 J·kg^{-1}.

Fig.4 shows the magnetic entropy changes (ΔS) of different specimens. The ΔT of specimen M_{AB} is 15.0 K, which is smaller than that of the superimposed specimen A and B ($T_{2B}-T_{1A}$=17.7 K). The ΔT of specimen M_{BCD} is 18.0 K, which is smaller than that of the superimposed specimen B, C, and D ($T_{2D}-T_{1B}$=22.0 K). The ΔT of specimen M_{ABCD} is 24.0 K, which is also smaller than that of the superimposed specimen A, B, C, and D ($T_{2D}-T_{1A}$=27.0 K).

Fig. 5 exhibits the temperature dependence of the adiabatic temperature change (ΔT_{ad}) at the magnetic strength of 0~1.5 T.

The max ΔT_{ad} is 2.25, 2.33, 2.65, 2.45, 2.24, 2.01, 2.30, 1.67, 1.89, and 1.42 K for specimen A, B, C, D, M_{AB}, M_{BC}, M_{CD}, M_{ABC}, M_{BCD}, and M_{ABCD}, respectively. It can be seen that the max ΔT_{ad} of four-component-bonded specimen M_{ABCD} is the smallest, but its cooling temperature zone is the widest, compared with those of other specimens, which is consistent with the magnetic entropy change results.

Fig.6 shows the compressive stress-strain curve of the four-component-bonded specimen M_{ABCD}. An obvious yield stage before reaching the maximum compressive strength of 157 MPa can be observed, which is appliable for the magnetic refrigerator as the magnetic refrigerant.

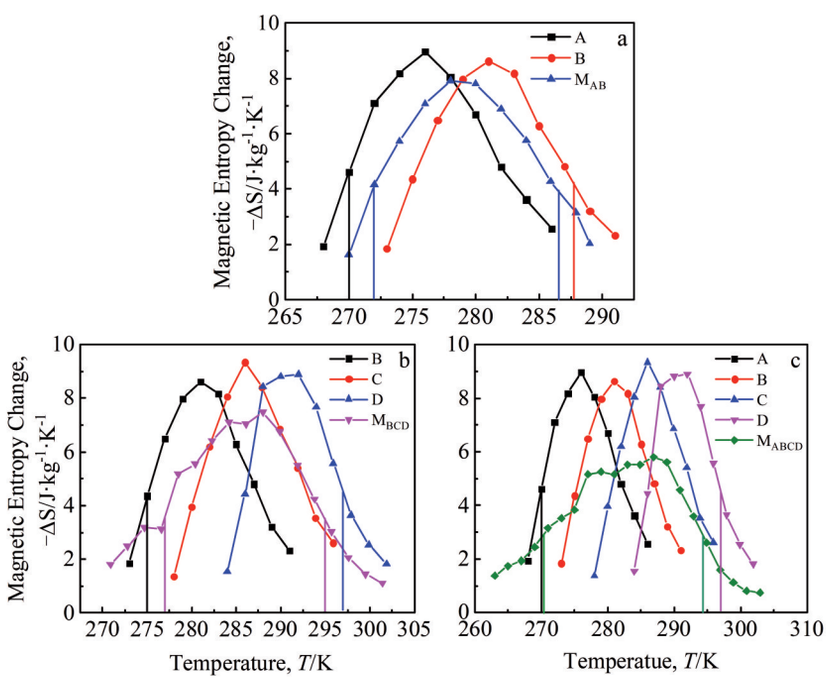

Fig.4 Magnetic entropy changes of different specimens at magnetic strength of 0~2 T: (a) specimens A, B, and M_{AB}; (b) specimens B, C, D, and M_{BCD}; (c) specimens A, B, C, D, and M_{ABCD}

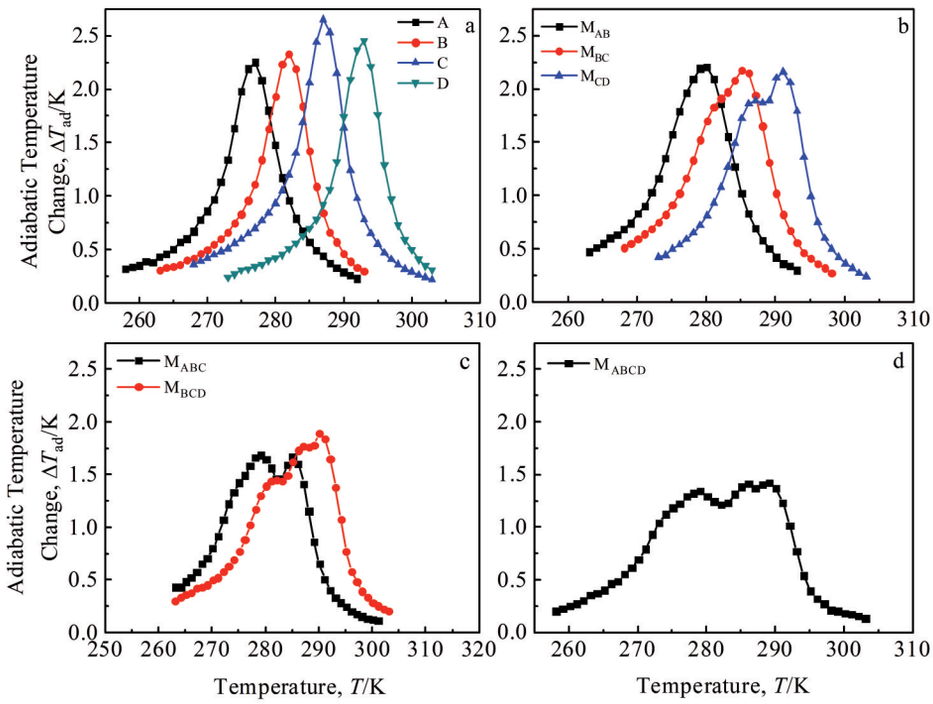

Fig.5 Relationships between adiabatic temperature change and temperature of different specimens at the magnetic strength of 0~1.5 T: (a) single-component specimens A~D; (b) two-component-bonded specimens M_{AB}, M_{BC}, and M_{CD}; (c) three-component-bonded specimens M_{ABC} and M_{BCD}; (d) four-component-bonded specimen M_{ABCD}

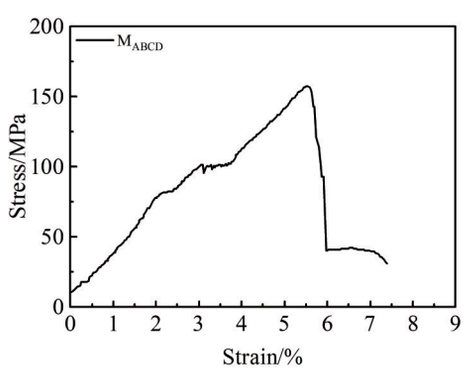

Fig.6 Compressive stress-strain curve of four-component-bonded specimen M_{ABCD}

3 Conclusions

1) The first-order magnetic transformation in the mix-bonded $La_{0.8}Ce_{0.2}Fe_{11.7-x}Mn_xSi_{1.3}H_{1.8}$ (x=0.23, 0.26, 0.29, 0.32) alloys is weakened, the hysteresis and magnetocaloric effect decrease, and the cooling temperature range is widened, compared with those of the single-component-bonded alloys.

2) The cooling temperature range of the four-component-bonded specimen is the widest, and its relative cooling power is optimal of 139.2 $J \cdot kg^{-1}$ among all the mix-bonded specimens.

3) The mix-bonding preparation of $La_{0.8}Ce_{0.2}Fe_{11.7-x}Mn_x$-$Si_{1.3}H_{1.8}$ alloy is an effective way to widen the cooling temperature range and to increase the relative cooling power.

References

1 Hu F X, Shen B G, Sun J R *et al. IEEE Transactions on Magnetics*[J], 2001, 37(4): 2328

2 Fujieda S, Hasegawa Y, Fujita A *et al. Journal Magnetism and Magnetic Materials*[J], 2004, 272-276(3): 2365

3 Fan Wenbing, Hou Yuhua, Huang Youlin *et al. Rare Metal Materials and Engineering*[J], 2019, 48(1): 323 (in Chinese)

4 Hu F X, Shen B G, Sun J R *et al. Applied Physics Letters*[J], 2001, 78(23): 3675

5 Balli M, Fruchart D, Gignoux D *et al. Journal of Physics-Condensed Matter*[J], 2007, 19(23): 236 230

6 Fukamichi K, Fujita A, Fujieda S *et al. Journal of Alloys and Compounds*[J], 2006, 408-412: 307

7 Lyubina J, Nenkov K, Schultz L *et al. Physical Review Letters* [J], 2008, 101(17): 177 203

8 Wang J W, Chen Y G, Tang Y B *et al. Journal of Alloys and Compounds*[J], 2009, 485(1-2): 313

9 Krautz M, Moore J D, Skokov K P *et al. Journal of Applied Physics*[J], 2012, 112(8): 83 918

10 Zimm C B, Jacobs S A. *Journal of Applied Physics*[J], 2013, 113(17): 17A908

11 Zhang H, Sun Y J, Niu E *et al. Applied Physics Letters*[J], 2014, 104(6): 62 407

12 Pan W J, Zhang H G, Xu L *et al. Journal of Magnetism and Magnetic Materials*[J], 2019, 476: 608

13 Zhang H, Liu J, Zhang M X *et al. Scripta Materialia*[J], 2016,

120: 58
14 Wang Y X, Zhang H, Liu E K *et al. Advanced Electronic Materials*[J], 2018, 4(5): 1 700 636
15 Pang W K, Chen Y G, Tang Y B *et al. Rare Metal Materials and Engineering*[J], 2017, 46(9): 2384
16 Liu Z G, Zhang Z Q, Ding Z *et al. Materialia*[J], 2019, 5: 100 170
17 Radulov I A, Karpenkov D Y, Skokov K P *et al. Acta Materialia* [J], 2017, 127: 389
18 Provenzano V, Shapiro A J, Shull R D *et al. Nature*[J], 2004, 429(6994): 853
19 Yamada H. *Physical Review B*[J], 1993, 47(17): 11 211
20 Pecharsky V K, Gschneidner K A. *Journal of Applied Physics*[J], 1999, 86(1): 565

复合粘结$La_{0.8}Ce_{0.2}Fe_{11.7-x}Mn_xSi_{1.3}H_{1.8}$磁工质的磁性能

程　娟[1]，刘翠兰[1]，张光睿[1]，孙乃坤[2]，张英德[1]，金培育[1]，黄焦宏[1]
(1. 包头稀土研究院 白云鄂博稀土资源研究与综合利用国家重点实验室，内蒙古 包头 014030)
(2. 沈阳理工大学 理学院，辽宁 沈阳 110159)

摘　要：采用中频感应炉制备$La_{0.8}Ce_{0.2}Fe_{11.7-x}Mn_xSi_{1.3}$母合金并退火，将合金饱和氢化后破碎成粉末。通过环氧树脂粘结，将居里温度T_C间隔为5 K的多种$La_{0.8}Ce_{0.2}Fe_{11.7-x}Mn_xSi_{1.3}H_{1.8}$（$x$=0.23，0.26，0.29，0.32，质量分数，%）合金粉末进行混合粘结，提高合金的磁熵半峰宽。用VersaLab和绝热温变直接测量仪测试粘结样品的磁性能。结果表明，与单一成分粘结样品相比，混合粘结样品的最大等温磁熵变有所降低，磁熵半峰宽以及相对制冷能力有所提高。含4种成分的混合粘结样品的相对制冷能力可以达到139.2 J/kg。

关键词：磁性材料；磁热效应；相对制冷能力；稀土

作者简介：程　娟，女，1984年生，硕士，高级工程师，包头稀土研究院白云鄂博稀土资源研究与综合利用国家重点实验室，内蒙古 包头 014030，电话：0472-5179355，E-mail：chengjuan@brire.com